AIAA SPACE 2012 Conference & Exposition
11 - 13 September 2012, Pasadena, California

AIAA 2012-5183

Rapid Cost Estimation for Space Exploration Systems

Dr. Dale C. Arney[1] and Dr. Alan W. Wilhite[2]
Georgia Institute of Technology/National Institute of Aerospace, Hampton, VA 23666

Incorporating cost estimation into the space system architecture design space exploration process enables decision-makers to qualitatively assess the cost impact of architecture decisions. By creating simple, system-level cost estimating relationships (CERs) derived from bottoms-up estimates of mass, this information can be incorporated in the decision-making process. The research presented in this paper develops these relationships for various system types based on a baseline configuration for each system type. The capability of these CERs are demonstrated by using them within a graph theory system architecture modeling framework to explore the options identified within the Exploration System Architecture Study (ESAS) mission modes comparison. These options, along with a commercial architecture that is significantly different than any of the options identified in ESAS are compared based on cost, and the overall system architecture comparison that includes all of the figures of merit used in ESAS are discussed.

Nomenclature

a	=	coefficient (first pound cost)
A	=	beta distribution parameter
b	=	coefficient (slope)
B	=	beta distribution parameter
C	=	system cost ($)
CDF	=	cumulative distribution function
Isp	=	specific impulse (sec.)
k	=	multiplicative factor for technology, system complexity, etc.
W	=	subsystem weight (pounds)
T	=	time (years)
T/W	=	thrust-to-weight ratio

I. Introduction

THE selection of space system architectures is highly dependent on several figures of merit, including but not limited to performance, cost, and risk. With budget constraints tightening around NASA's human exploration program, developing a system architecture that provides cost savings over alternatives is crucial to accomplishing meaningful missions in human space exploration. However, often cost estimating during the architecture generation phases of conceptual design requires a more detailed understanding of the configuration and technology selection for each individual system than is available. Top-down system sizing tools, which are frequently used in rapid system architecture design space exploration, often do not provide detailed breakdowns of the mass, power, and complexity of each subsystem.

The research presented in this paper develops a set of Cost Estimating Relationships (CERs) that require only basic information from the system sizing tools. For propulsive stages, information such as dry mass and propellant type are required to estimate both the development and the flight unit cost. Other systems only require the dry mass, as a configuration is assumed based on previous designs, and new systems are assumed to be similar. This system-level CER provides the capability to incorporate cost into the space system architecture design space exploration and decision-making process.

[1] Research Engineer II, 100 Exploration Way, AIAA Student Member.
[2] Samuel P. Langley Distinguished Professor, 100 Exploration Way, AIAA Associate Fellow.

II. Background and Methodology

The Life Cycle Cost (LCC) of a space system is the total cost of a project across all phases, including design, development, production, operations, and disposal. The cost to develop a system from concept to a complete design that is ready for production is categorized as Design, Development, Testing, and Evaluation (DDT&E) cost. The cost to produce a system for use in the mission is the flight unit cost. Both of these costs are typically predicted during the conceptual design phase as a function of mass and system complexity [1]. The operations and disposal costs depend on drivers that are not always clearly linked to the system architecture, but rather indirect factors such as ground logistics and workforce management [2]. Finally, launch cost is dependent upon launched mass and launch vehicle cost, which varies based on the launch vehicle used in the system architecture.

A Cost Estimating Relationship (CER) for a given subsystem is a parametric regression on the cost of analogous systems based upon the weight of the subsystem of the form presented in Equation (1).

$$C = k \cdot aW^b \tag{1}$$

where C is the subsystem cost, k is a complexity factor associated with multipliers based on certain design decisions (technology development, manufacturing methods, etc.), and a and b are constants defined by the regression on the analogous system. CER's are well suited to low-fidelity, rapid comparisons of space systems [3].

The NASA/Air Force Cost Model (NAFCOM) is a parametric cost-estimating tool that contains multiple, subsystem-level CERs based on the Resource Data Storage and Retrieval (REDSTAR) database of historical spacecraft, launch vehicles, and rocket engines [4]. Along with subsystem weight, NAFCOM uses metrics to determine the complexity factor to apply to the CER. These metrics are Manufacturing Methods, Engineering Management, New Design, Funding Availability, Test Approach, Integration Complexity, Pre-Development Study, and other subsystem-specific metrics. The total system cost is then computed as the sum of the subsystem costs plus integration and management costs [4].

Transcost is another cost estimating tool for use with launch vehicles, but uses CER's on total system mass to predict a total system DDT&E and flight unit cost [5]. This formulation is useful to estimate the cost for conceptual systems that may not have fully-defined subsystem details. The complexity factor applied to the CER is dependent upon the system type (liquid and solid propulsive stages, crew modules, etc.) and consists of metrics such as system uniqueness, team experience, and vehicle mass fraction. An example Transcost CER for the DDT&E cost of an expendable, liquid-propulsion launch vehicle stage is shown in Figure 1 [5].

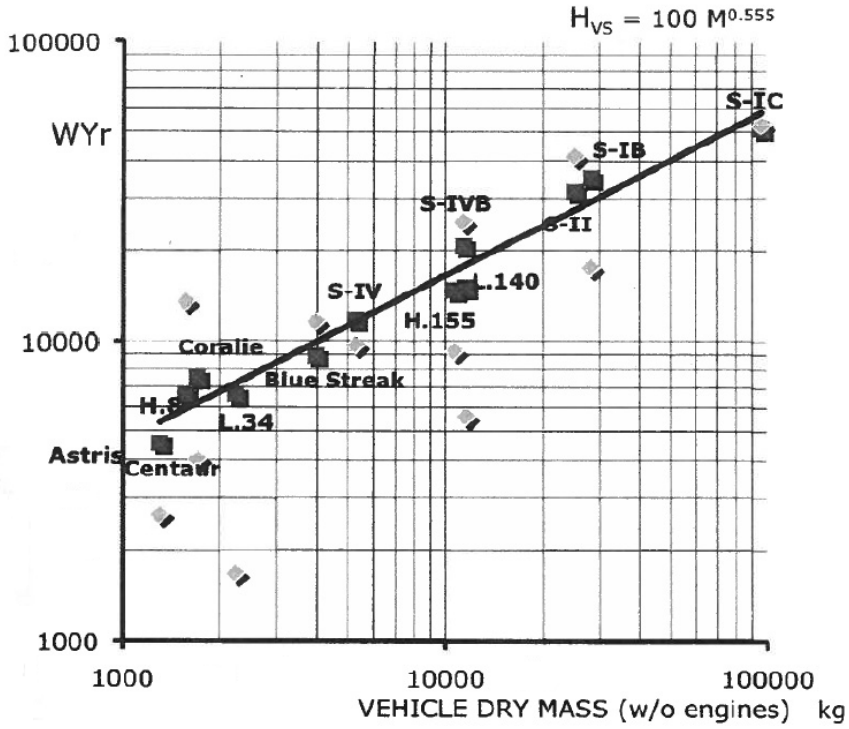

Figure 1: Transcost CER for Expendable, Liquid-Propulsion Launch Vehicle Stage [5]

The costs associated with DDT&E do not occur within a single year. Therefore, these costs are distributed over multiple years through the use of a beta distribution curve. This distribution, developed at Johnson Space Center (JSC) in the 1960s, is used to spread parametrically derived cost estimates over the duration of the development process [1]. This percentage of total cost spent up to a certain time is defined by a Cumulative Distribution Function (CDF), which holds the form presented in Equation (2).

$$CDF = 10T^2(1-T)^2(A+BT) + T^4(5-4T) \tag{2}$$

Here, T is the fraction of time of the entire DDT&E period ($0 \leq T \leq 1$), and A and B are distribution parameters such that $0 \leq A + B \leq 1$. In the case where $A = 0$ and $B = 1$, 50 percent of the cost is spent after 50 percent of the time has passed (called a 50:50 spread). In the case where $A = 0.32$ and $B = 0.68$, 60 percent of the cost is spent after 50 percent of the time has passed (called a 60:40 spread) [6]. Standard practice at NASA is to use a spread that commits more money early in the development period (e.g. 60:40 spread) for technically challenging designs and manned systems, while a 50:50 spread is adequate for systems with significant heritage or less demanding technical challenges [1].

III. Cost Estimating Relationships

Estimates of the DDT&E and flight unit costs for each system type must be at a level of fidelity consistent with the sizing methods during the conceptual system architecture formulation in order to incorporate cost in the decision-making. These conceptual system sizing tools use existing or previously analyzed spacecraft as bases for the mass estimates of future systems. This section provides an overview of the sizing methodology for the system types utilized in this analysis. These mass estimating tools provide estimates of subsystem masses based on the vehicle configuration, performance requirements, and other metrics. That mass breakdown and configuration is then used to generate bottoms-up cost estimates using NAFCOM. By varying the inputs, the subsequent mass estimates are used to generate multiple cost estimates for varying system masses. This set of cost estimates for the various system masses are then used to create a system-level cost estimating relationship that only relies on the dry mass of the system in question.

A. Mass Estimation

For each of the system types presented in this section, the overall system mass is a build-up of subsystem masses. These masses vary for each system type, but in general include structure, protection (thermal, radiation, etc.), propulsion, power, avionics, and environmental (life support, crew systems, etc.). System models either use photographic scaling of subsystems (physics-based scaling of systems proportionally with respect to a baseline system based on the new system requirements) [7].

The crew capsule model uses a photographically scaled version of the Block 2 Lunar Crew Exploration Vehicle presented in the Exploration System Architecture Study (ESAS) [8] based on the number of crew and stay time. This system was volumetrically sized to accommodate a crew of six for a mission to the ISS, but the crew accommodations and life support consumables are for a crew of four to perform the lunar mission. Also, the thermal protection system is designed to accommodate lunar reentry velocity. The geometry for this vehicle is presented in Figure 2.

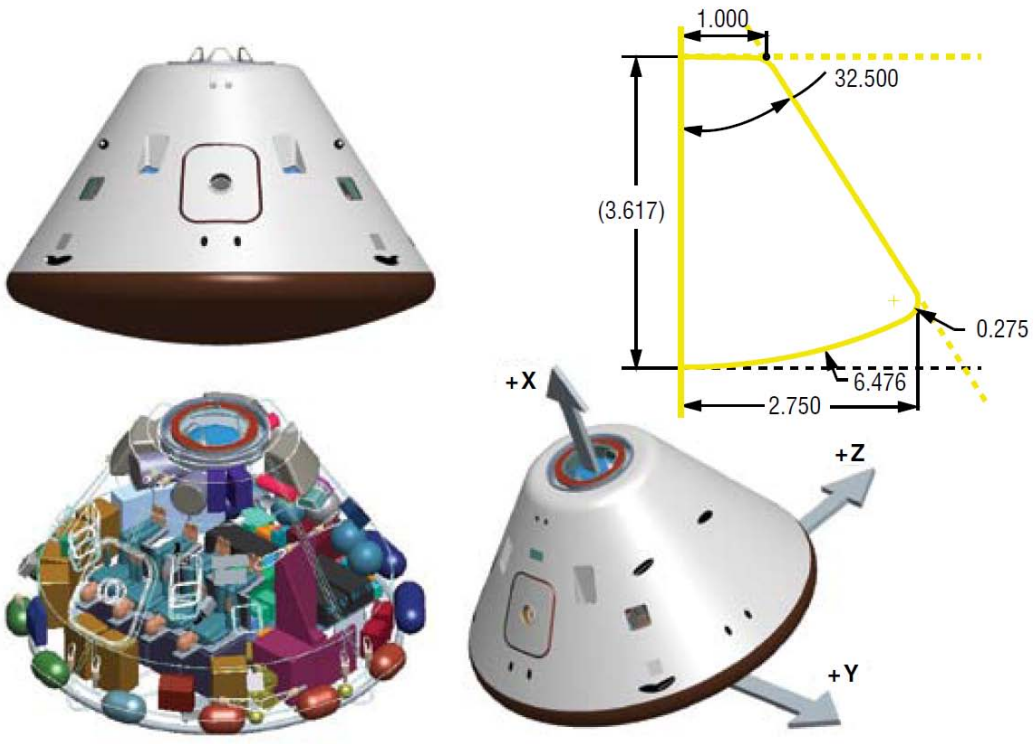

Figure 2: Configuration of Block 2 Lunar Crew Exploration Vehicle [8]

The lunar descent stage model uses photographic scaling of two separate vehicles depending on the propellant type. Descent stages that use cryogenic propellant, such as LOX/LH2 or LOX/CH4, are based on the descent stage for the Lunar Surface Access Module (LSAM) presented in ESAS [8]. The geometry for this vehicle is presented in Figure 3. Descent stages that use storable propellant, such as NTO/MMH, are based on the descent stage for the Apollo Lunar Excursion Module [9]. The geometry for this vehicle is presented in Figure 4.

Figure 3: Configuration of ESAS LSAM Cryogenic Descent Stage [8]

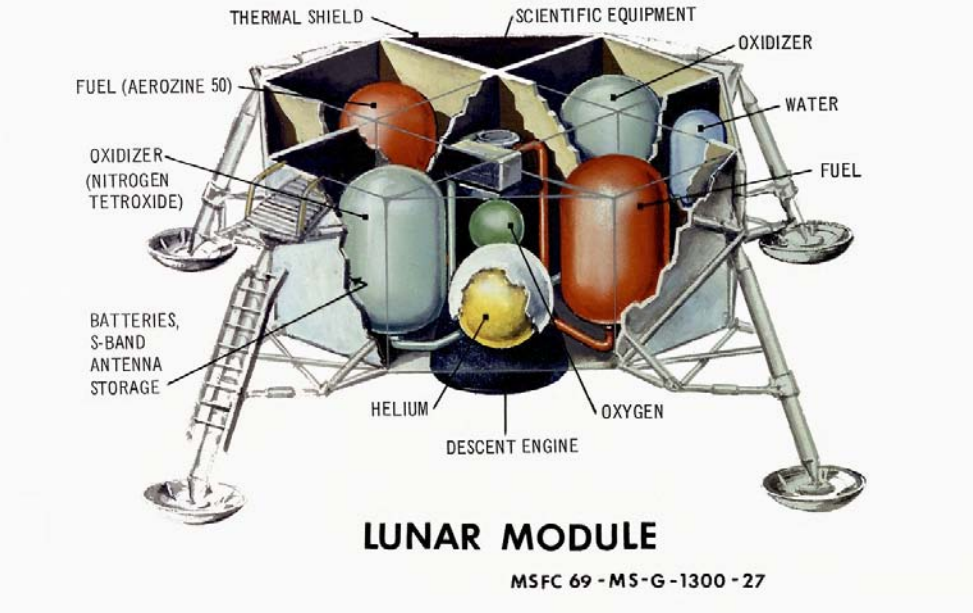

Figure 4: Configuration of Apollo Lunar Excursion Module Hypergolic Descent Stage (Image: NASA)

The lunar ascent stage model uses a photographically scaled model of the propulsive elements of the LSAM ascent stage. Figure 5 presents the full LSAM ascent stage including the surface habitat. The surface habitat is excluded from the ascent stage analysis, and is modeled separately. Changes in performance requirements (ΔV, T/W, and payload mass) and system implementation (propellant type) affect the sizing of the structure, protection, and propulsive system masses.

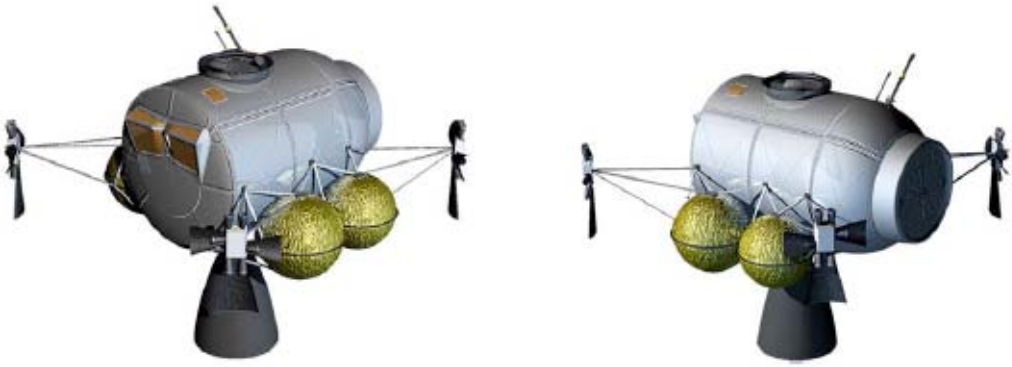

Figure 5: Configuration of ESAS LSAM Lunar Ascent Stage and Surface Habitat [8]

The surface habitat model is a photographically scaled version of the surface habitat used on the LSAM from ESAS, as presented previously in Figure 5. The habitat scales with number of crew and stay time. The pressure vessel, power, life support system, consumables, and thermal control systems scale with the ratio of total crew days. Crew accommodations scale with the number of crew, and the avionics system remains constant.

The propulsive stages are sized by combining regressions for subsystems of existing propulsive stages. These bottoms-up estimates are validated with baseline systems, such as the service module and Earth departure stage from ESAS [8]. The inputs for the propulsive stage are ΔV (for each burn), payload mass (for each burn), propellant combination (fuel, oxidizer, oxidizer-to-fuel ratio), and system T/W. The subsystem masses are based on existing upper stages and in-space stages [8],[10]. Systems with a propellant mass below 20,000 kg are modeled as service module configurations, while systems above 20,000 kg of propellant are modeled as upper stages or in-space stages. The difference in these two configurations can be seen in Figure 6 [8]. Propellant depots are modeled similarly to the propulsive stages, as they include the same subsystems, such as tanks, thermal protection, power, and propulsion.

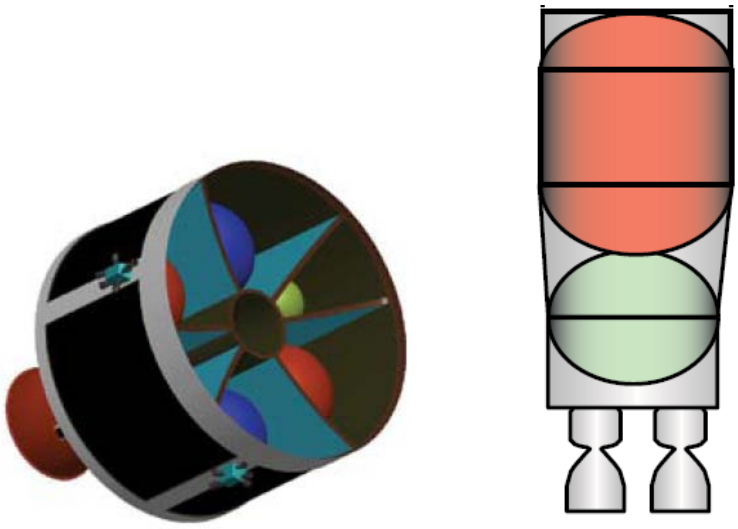

Figure 6: Configurations of Service Module (left) and Earth Departure Stage (right) (not to scale) [8]

Finally, the in-space habitat is a photographically scaled version of the deep space habitat developed for the Human Exploration Framework Team [11] to support a crew of four for 365 days. The geometry of this habitat is presented in Figure 7. This system scales with number of crew and mission duration. While this system is not necessarily used in the lunar space system architecture, it would be required for missions to destinations such as near-Earth asteroids.

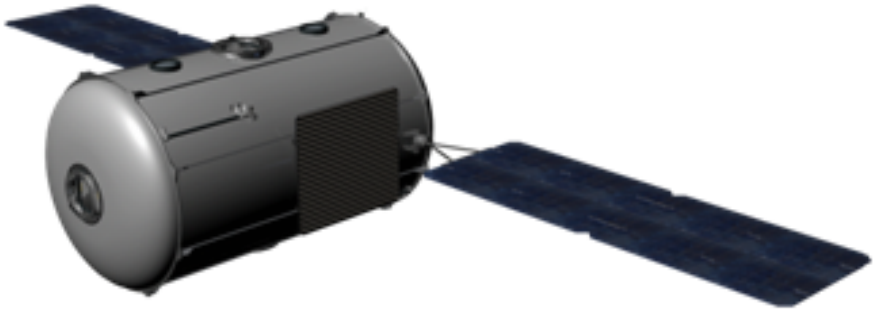

Figure 7: Configuration of Deep Space Habitat [11]

B. Cost Estimation

With the configuration and subsystem mass computed with the sizing tools, NAFCOM is able to produce a bottoms-up estimate of DDT&E and flight unit costs (in FY12 dollars). In addition to the subsystem mass, NAFCOM uses metrics to determine the complexity factor to apply to the CER, which are specific to the given system type. The total system cost is then computed as the sum of the subsystem costs plus integration and management costs. The exception is the launch vehicle system type, which used Transcost estimates that were specifically developed for launch vehicles and listed prices for existing commercial launch vehicles. System-level regressions for the DDT&E and flight unit costs were developed for a range of dry masses for each system type. The regressions are of the form of the CER in Equation (1), with the coefficients presented in Table 1. Figure 8 – Figure 14 present these CERs in graphical form. Only the cryogenic models are presented in the figures, as the trends (power of the CER) are assumed to be similar for both types of propellant, but the first pound cost (coefficient of the CER) is higher for cryogenic systems than it is for storable systems. Also, the DDT&E CER predicted both propellant types within a reasonable level of uncertainty, while the flight unit CER indicated a distinct cost difference between the two propellant types.

Table 1: CER Coefficients for Each System Type

System Type	DDT&E Cost CER Coefficients		Flight Unit Cost CER Coefficients	
	k·a	b	k·a	b
Crew Capsule	285.57	0.2667	49.923	0.2409
Descent Stage (Cryogenic)	168.22	0.3152	6.8608	0.4146
Descent Stage (Storable)	168.22	0.3152	4.8935	0.4146
Ascent Stage (Cryogenic)	405.62	0.2151	92.715	0.1606
Ascent Stage (Storable)	405.62	0.2151	66.129	0.1606
Surface Habitat (4 crew)	751.64	0.1183	124.32	0.1402
In-Space Habitat (4 crew)	1457.7	0.0856	46.624	0.2146
Propulsive Stage (Cryogenic)	29.125	0.4554	2.6147	0.4782
Propulsive Stage (Storable)	29.125	0.4554	1.8650	0.4782
Propellant Depot	75.492	0.3566	11.487	0.3175

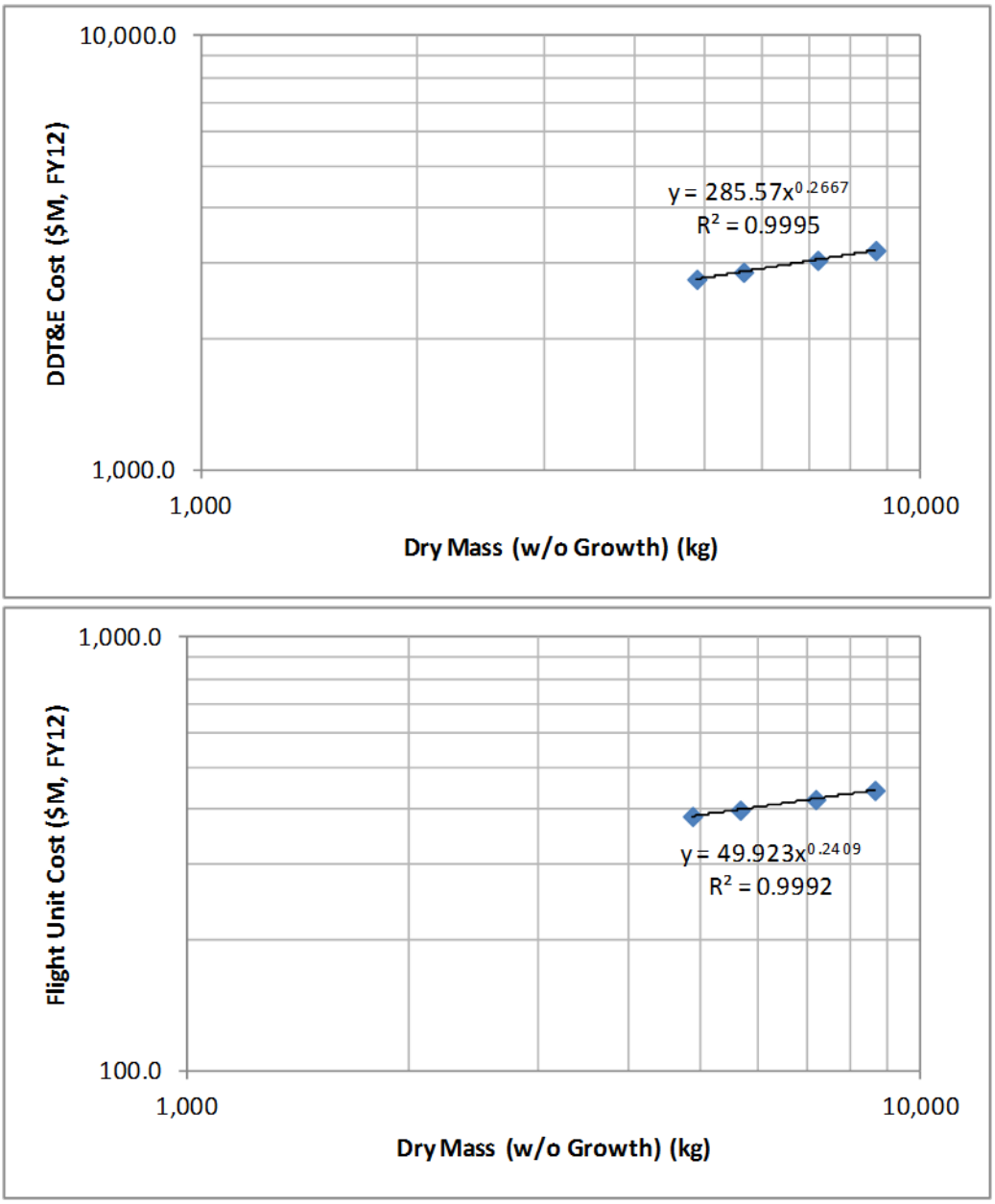

Figure 8: Crew Capsule CER for DDT&E Cost (Top) and Flight Unit Cost (Bottom)

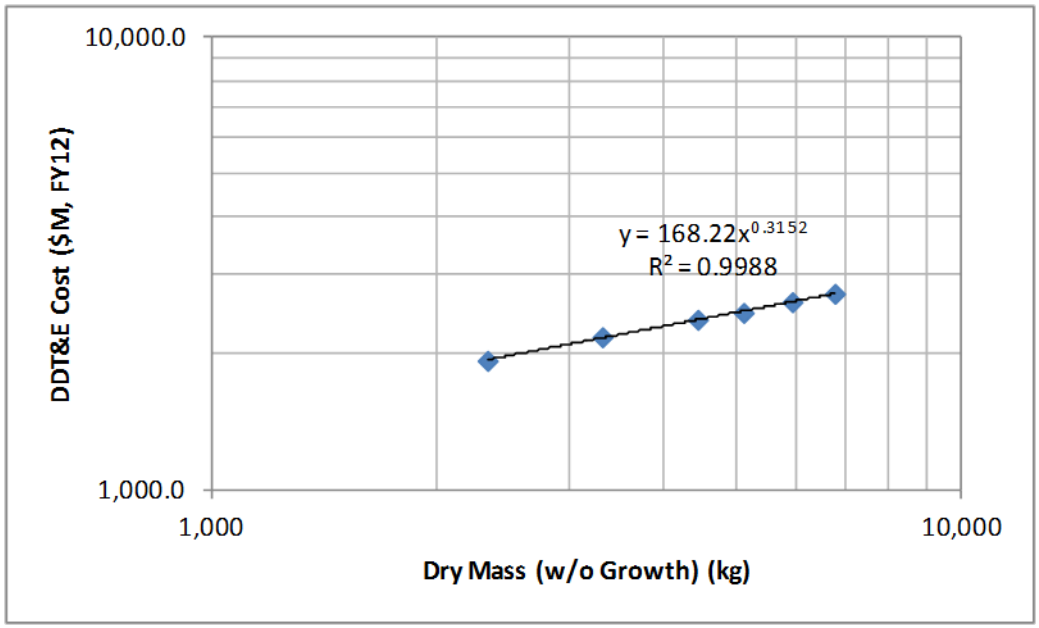

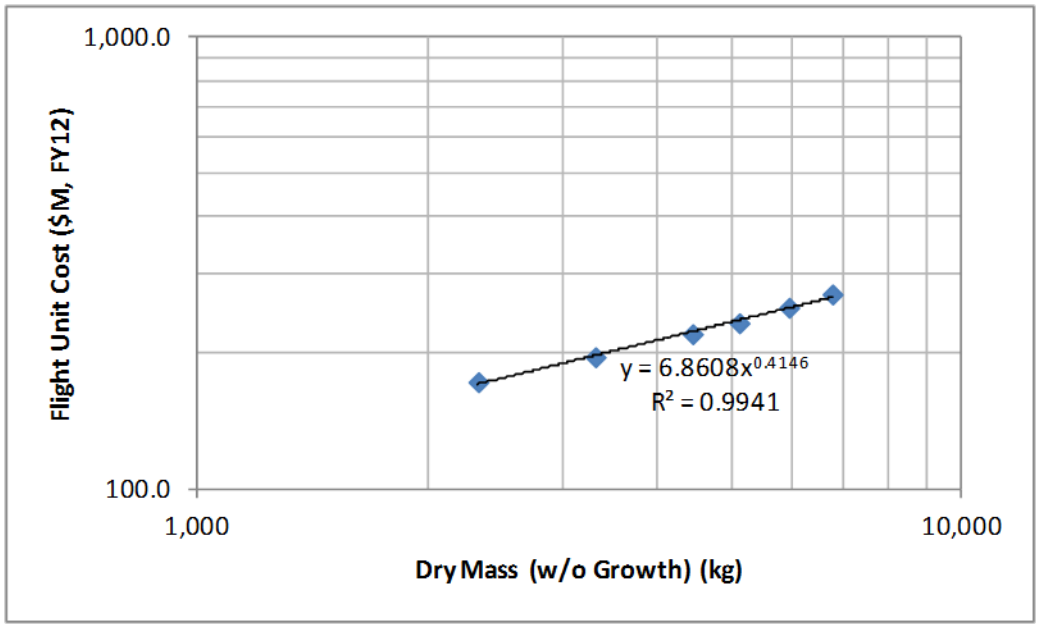

Figure 9: Cryogenic Lunar Descent Stage CER for DDT&E Cost (Top) and Flight Unit Cost (Bottom)

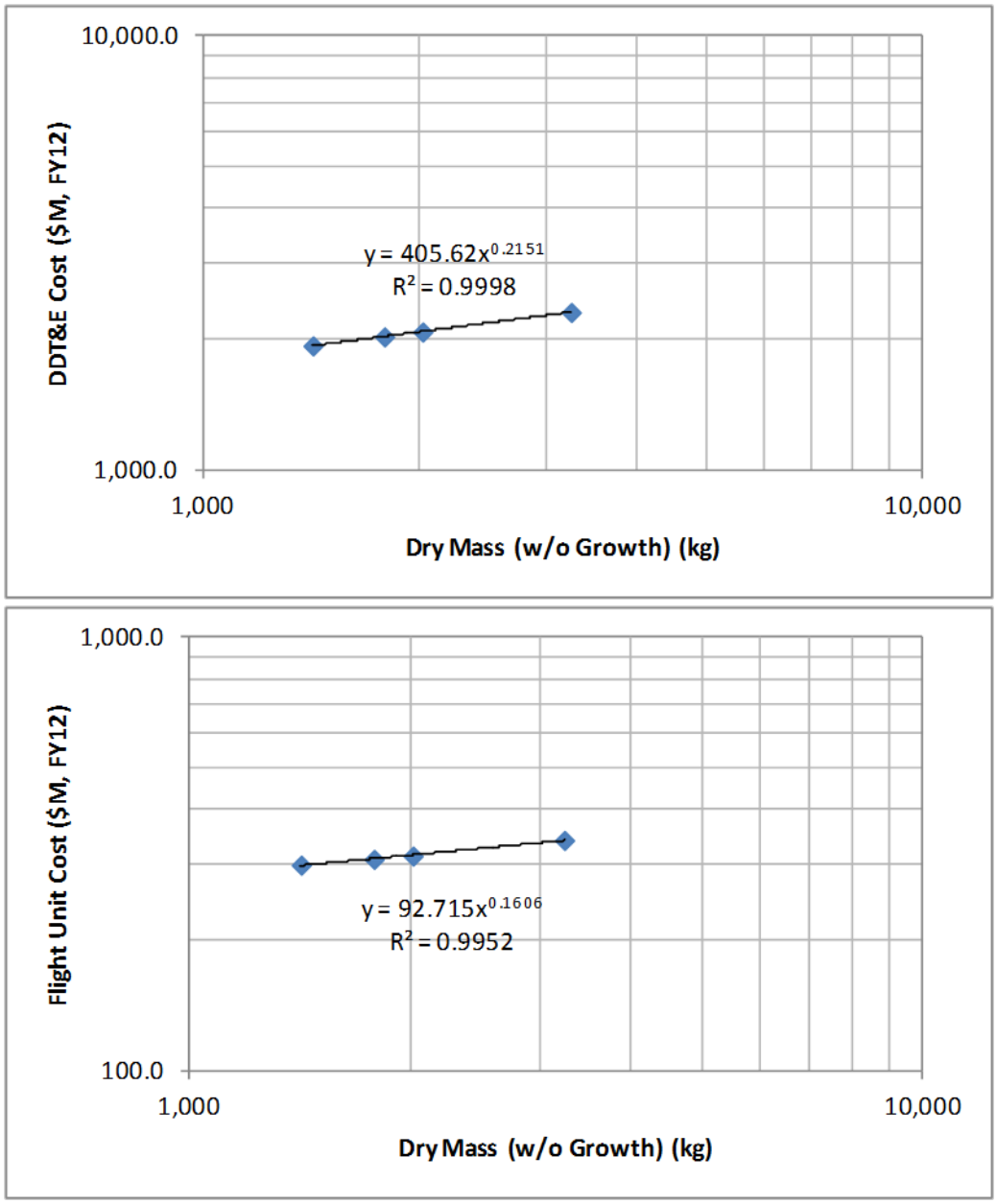

Figure 10: Cryogenic Lunar Ascent Stage CER for DDT&E Cost (Top) and Flight Unit Cost (Bottom)

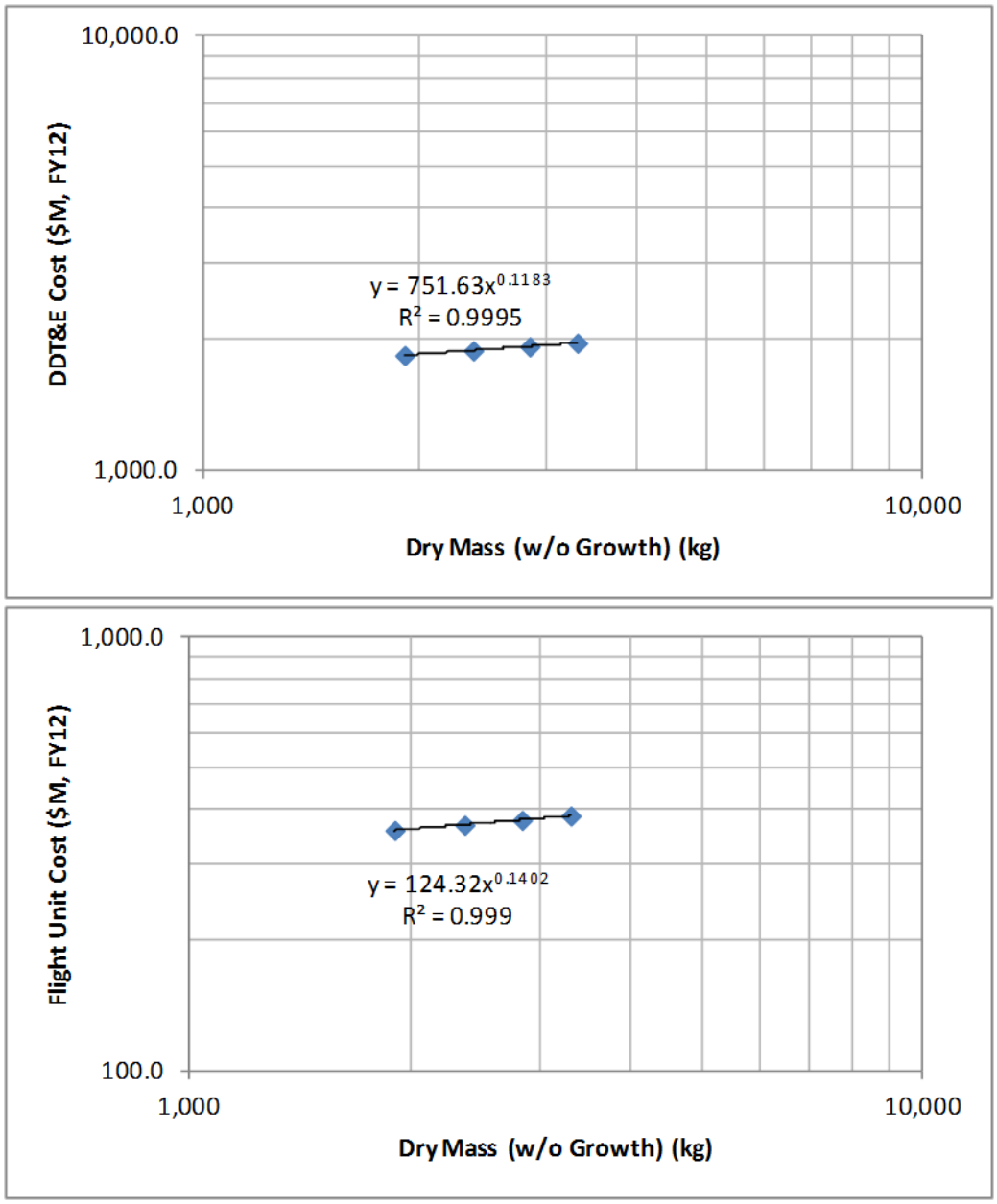

Figure 11: Surface Habitat CER for DDT&E Cost (Top) and Flight Unit Cost (Bottom)

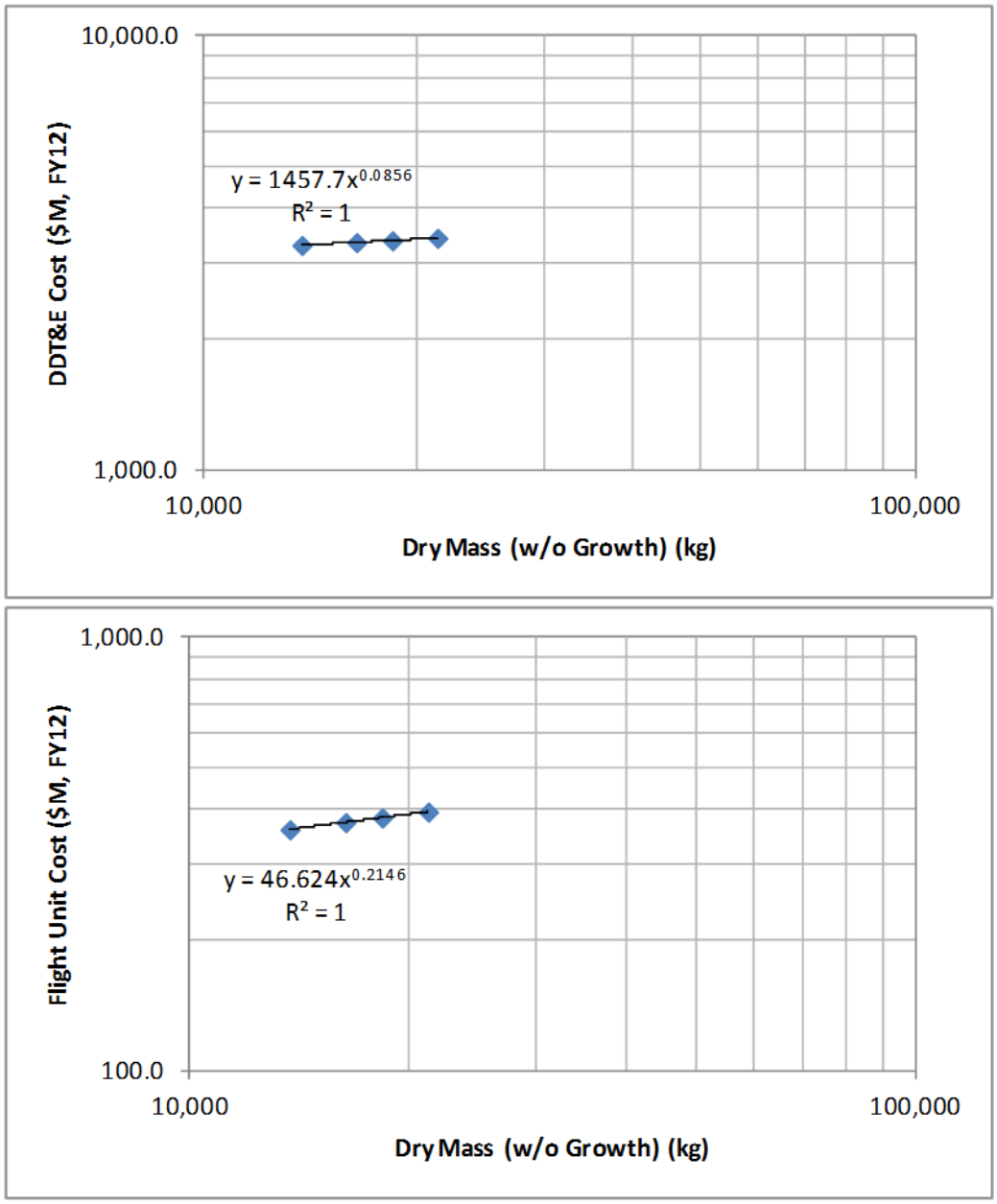

Figure 12: In-Space Habitat CER for DDT&E Cost (Top) and Flight Unit Cost (Bottom)

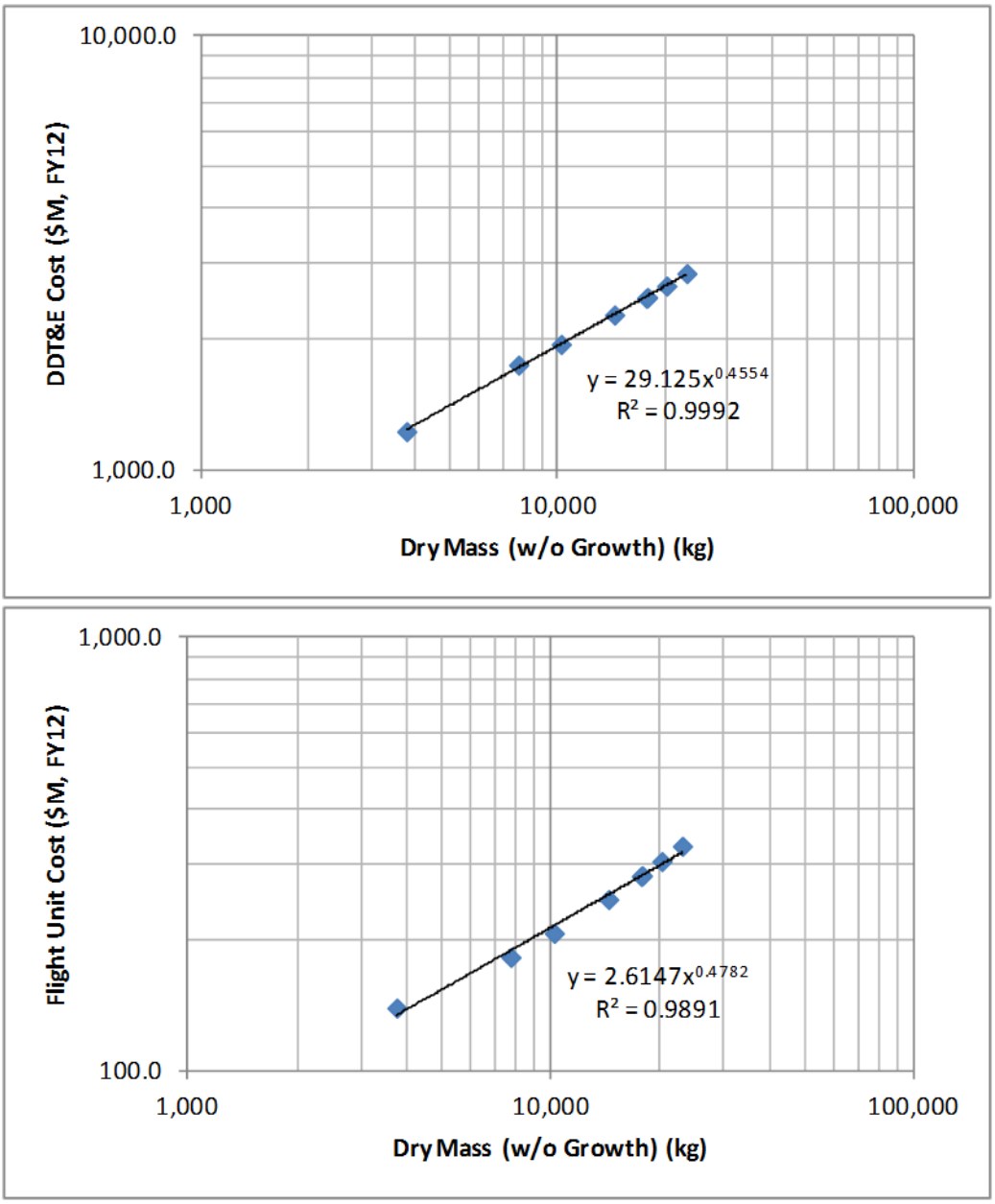

Figure 13: Cryogenic Propulsive Stage CER for DDT&E Cost (Top) and Flight Unit Cost (Bottom)

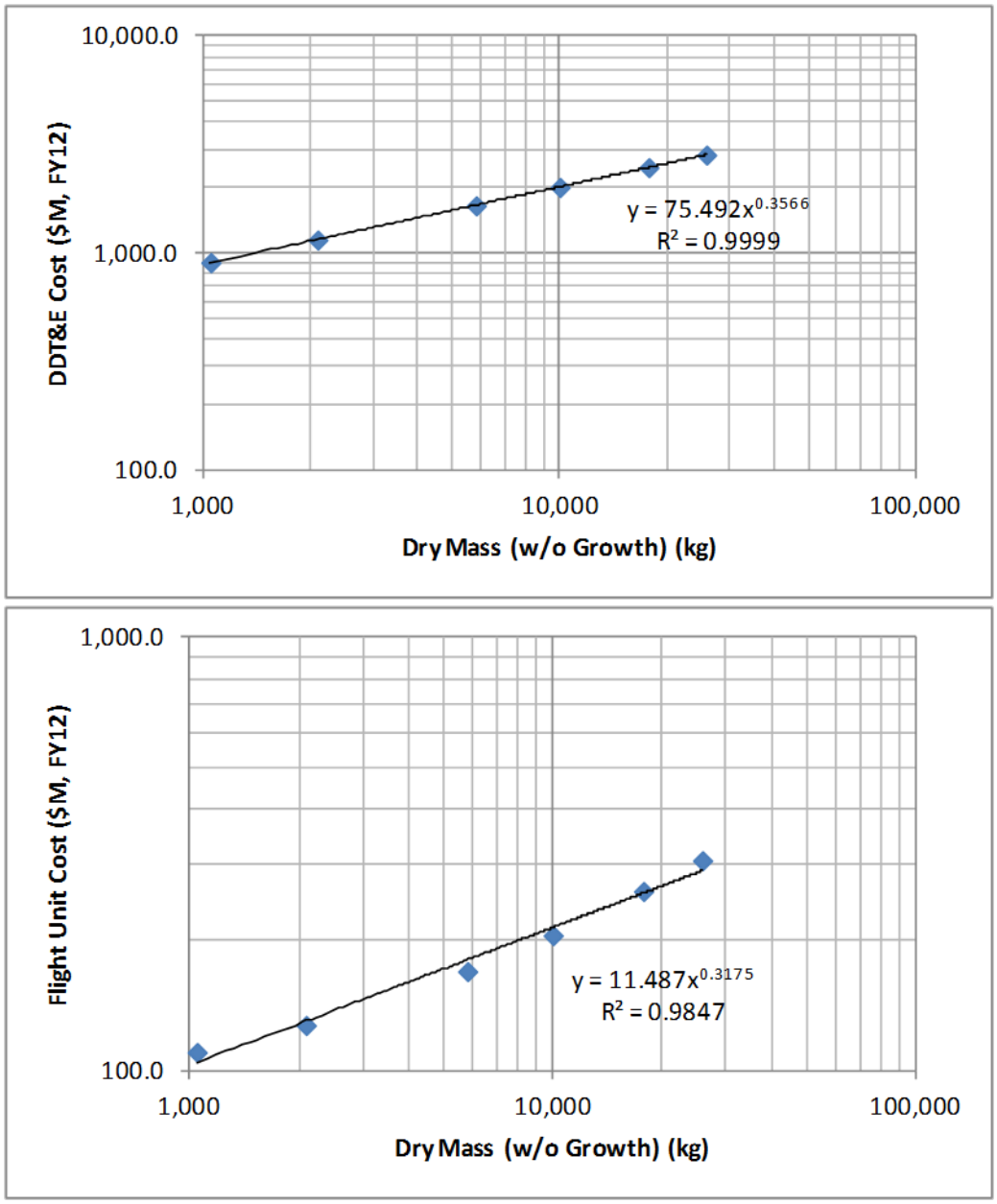

Figure 14: Propellant Depot CER for DDT&E Cost (Top) and Flight Unit Cost (Bottom)

The results of the Transcost calculation for Heavy Lift Launch Vehicles (HLLVs) are presented in Table 2, along with the price for the commercial launch vehicles included in the analysis. The Transcost regressions [5] were anchored to a launch vehicle similar to the Cargo Launch Vehicle, the HLLV presented in ESAS [8], [12]. To model various payload capabilities, this launch vehicle was photographically scaled, and the estimates of subsystem masses, DDT&E cost, and flight unit costs were estimated. The cost estimates are given for deliveries to both LEO and to a suborbital point, which excludes the cost of an upper stage. This upper stage would be accounted for in the propulsive stage that performs the suborbital burn. The commercial launch vehicles assume that there is no DDT&E cost, and the flight unit cost is the price of purchasing a launch vehicle, as reported by the provider [12],[13].

Table 2: Launch Vehicle Cost Model Results Overview

Launch Vehicle	Delivery to Low Earth Orbit			Delivery to Suborbital Point		
	Payload (mt)	DDT&E Cost (FY12, $M)	Flight Unit Cost (FY12 $M)	Payload (mt)	DDT&E Cost (FY12, $M)	Flight Unit Cost (FY12, $M)
29 mt Crew LV	29	5,502	892	--	--	--
70 mt HLLV	70	13,274	1,551	136	11,004	1,295
100 mt HLLV	100	14,731	1,989	194	12,252	1,663
130 mt HLLV	130	16,746	2,796	251	14,066	2,401
150 mt HLLV	150	18,222	3,472	290	15,413	3,032
Delta IV-H	24	0	318	--	--	--
Falcon Heavy	53	0	135	--	--	--

Finally, estimating the cost of propellant delivery for architectures that utilize on-orbit refueling uses a cost-per-kilogram metric. The current price of existing commercial launch vehicles is $14,286/kg (based on a Delta IV-H). The projected price for commercial launch vehicles in the future is $2,358/kg (based on a Falcon Heavy). The inclusion of both of these options allows the system architect to view the difference between current capability and projected future capability.

C. System Architecture Modeling

To model space system architectures in a manner that enables rapid analysis of various system architecture options, graph theory is used [7]. Graph theory presents the mathematical representation of these graphs in terms of an adjacency matrix (links the nodes together) and an incidence matrix (links edges to nodes) [14]. In space systems architecting, expressing the physical locations (Low Earth Orbit (LEO), Low Lunar Orbit (LLO), etc.) and steady states (interplanetary trajectory) as nodes and the different means of moving between the nodes (propulsive maneuvers, entry methods, etc.) as edges formulates a mathematical representation of the architecture-level design space. The representation of a lunar system architecture design space is presented in Figure 15, with nodes defined in Table 3 (Link Group Numbers represent locations where assets can be pre-deployed) [7].

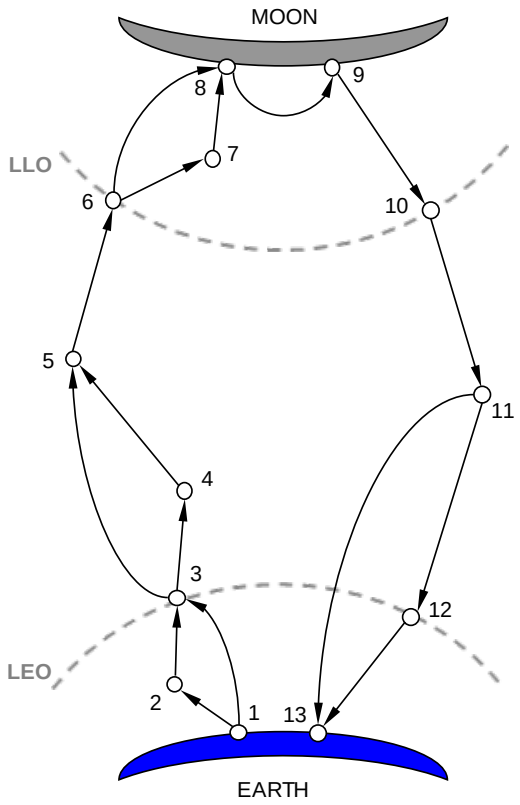

Figure 15: Lunar System Architecture Design Space Represented as a Graph [7]

Table 3: Lunar Mission Node Definition [7]

Node No.	Node Name	Link Group No.
1	Earth Surface (Outbound)	
2	Suborbital Staging Point	
3	LEO (Outbound)	1
4	LEO Propellant Depot	
5	Trans-Lunar Trajectory (Outbound)	
6	LLO (Outbound)	2
7	Lunar Braking Point	
8	Lunar Surface (Arrival)	3
9	Lunar Surface (Departure)	3
10	LLO (Return)	2
11	Trans-Lunar Trajectory (Return)	
12	LEO (Return)	1
13	Earth Surface (Return)	

The selection of a given system architecture using graph theory involves defining the paths that each system takes through the space system architecture graph. A path through the graph is defined as a list of edges that are traversed, which in turn defines the nodes visited and functions performed by each system. This mapping completely defines the given space system architecture concept, defining all functions of each system and the interrelationships between systems. This mapping is subject to certain rules that ensure feasibility (crew must travel with a habitat, propulsive burns must have a propulsive stage, etc.) [7].

Once the system map has been constructed, the mass and cost of each system must be determined so that different system architecture options can be compared. Systems that cohabitate a given edge in the architecture graph have a relationship. The system hierarchy, or order in which those systems are sized, is determined through a "topological sort," which links the relationships between systems in the system map to the system hierarchy. The level of fidelity of each system sizing model must enable rapid evaluation of the performance and cost. Therefore, first order methods such as response surfaces, regressions of historical data, and photographic scaling of existing systems are used [15]. However, the modular nature of the system hierarchy allows higher fidelity models to be used for any system within the architecture without altering the architecture selection methodology [7]. Cost estimates are produced using the system-level cost estimating relationships derived in the previous section.

IV. System Architecture Design Space Exploration

A. Architecture Design Space Overview

In January 2004, President George W. Bush, through the issuance of the Vision for Space Exploration, provided a goal for NASA to return humans to the Moon by 2020. In response to this direction, the Exploration Systems Architecture Study (ESAS) explored several options for achieving this goal [8].

ESAS identified the various mission modes that existed in the design space, as shown in Figure 16. The modes were split into the taxonomy based on whether or not there was a rendezvous in Earth orbit, lunar orbit, both, or none. The Apollo mission utilized a Lunar Orbit Rendezvous (LOR) without Earth Orbit Rendezvous (EOR). Other

combinations include EOR only (also known as EOR-Direct), LOR only, and EOR-LOR, which ESAS deemed the best solution with respect to a set of figures of merit that included safety, performance, extensibility/flexibility, risk, and affordability [8].

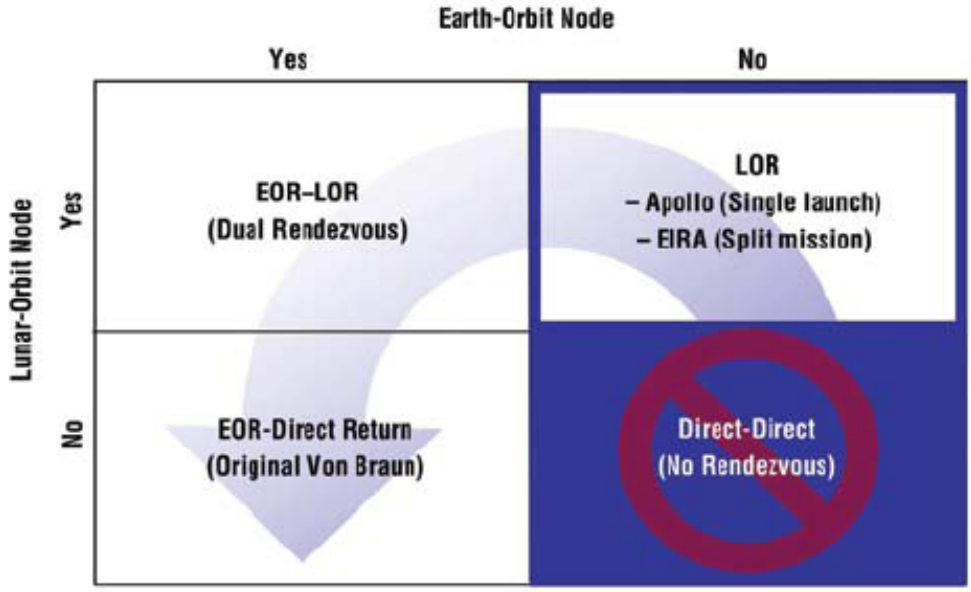

Figure 16: ESAS Lunar Mission Mode Taxonomy [8]

These options fit within the lunar system architecture design space graph presented in Figure 15 and Table 3. To explore the same modes for the lunar design space defined by the graph, the system architect defines different paths for systems to take within that graph. The various options defined by ESAS in Figure 34 are enumerated in the subsequent pages, along with an option that is dissimilar to the ESAS system architectures, which will demonstrate the flexibility of the modeling framework and rapid cost estimation.

Throughout the analysis of this system architecture design space, several systems are given acronyms to denote their primary function. Table 4 presents a summary of these systems, including the full name, acronym, system type (defining the sizing tool used), and potential functions that these systems perform in the various system architecture alternatives. The Earth Departure Stage (EDS) is a propulsive stage that performs large propulsive burns, such as Trans-Lunar Injection (TLI) or Lunar Orbit Insertion (LOI), and has a large propellant capacity. The Lunar Surface Access Module (LSAM) is divided into three systems that provide the three functions that are required for lunar surface access: planetary descent, surface habitation, and planetary ascent. There is flexibility in the functionality of these stages as the descent stage can also perform LOI, the ascent stage can also perform Trans-Earth Injection (TEI), and the surface habitat can be removed in lieu of a crew capsule. The Crew Exploration Vehicle (CEV) consists of two systems: a Command Module (CM), which is the crew capsule that provides habitation in space or on the surface to replace the surface habitat, and provides Earth entry capability; and a Service Module (SM) which is a propulsive stage that performs the TEI burn. The SM is a small stage that has multiple tanks positioned radially while the EDS has two large tanks positioned axially. This differentiation is automatically made within the sizing tool based on propellant load. Also, while these system names are used throughout in different architectures, the size and propellant usage are typically not equal for each instance.

Table 4: Overview of Systems Used in ESAS Mission Modes Comparison

System Name	Acronym	System Type	Potential Function(s)
Earth Departure Stage	EDS	Propulsive Stage	TLI, LOI
Lunar Surface Access Module	LSAM	Lunar Descent Stage	LOI, Planetary Descent, Planetary Ascent
		Lunar Ascent Stage	Planetary Ascent, TEI
		Surface Habitat	Crew Habitation (surface)
Crew Exploration Vehicle Command Module	CEV CM	Crew Capsule	Crew Habitation (in-space or surface), Earth Entry
Crew Exploration Vehicle Service Module	CEV SM	Propulsive Stage	TEI

The first system architecture, presented in Figure 17, is the LOR-LOR system architecture. The first launch delivers an Earth Departure Stage and a two-stage LSAM to LEO using a Heavy Lift Launch Vehicle (HLLV). The EDS performs the TLI and LOI burns. The LSAM (which consists of a surface habitat, an ascent stage, and a descent stage) loiters in LLO. The next launch delivers an EDS and the crew in the CEV command module and the service module. Again, the EDS performs the TLI and LOI burns. The crew rendezvous in LLO with the LSAM, and descends to the surface while the CEV remains in LLO unmanned. After the surface mission, the crew ascends to the CEV and discards the ascent module of the LSAM. The CEV SM then performs the TEI burn to return directly to Earth. In this and all subsequent architectures, the standard EDS and LSAM descent module use Liquid Oxygen/Liquid Hydrogen (LOX/LH2) propellant, and the LSAM ascent module and CEV service module use Liquid Oxygen/Liquid Methane (LOX/CH4) propellant. Within the present framework, this implementation can be easily changed to explore more of the design space.

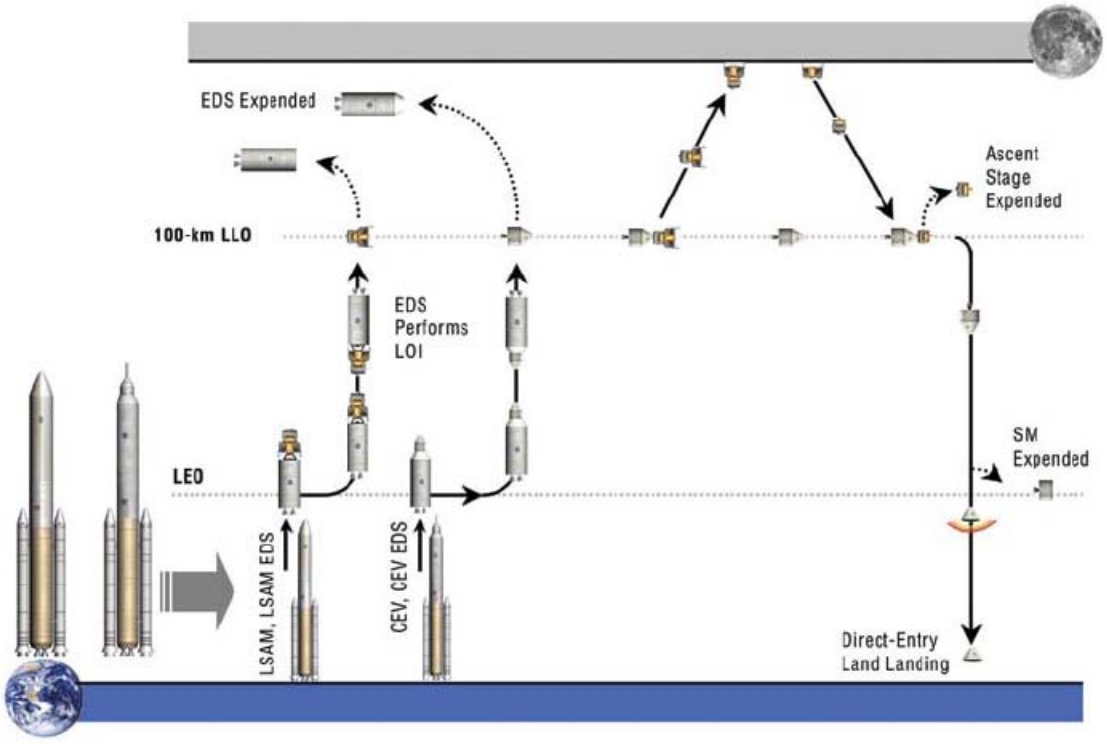

Figure 17: LOR-LOR Lunar System Architecture Option [8]

The second system architecture, presented in Figure 18, is an EOR-LOR system architecture that utilizes two different sized launch vehicles: one to deliver the cargo, and one to deliver the crew. The first launch delivers the EDS and LSAM to LEO using the cargo launch vehicle. The EDS also performs suborbital burning to reach LEO, where the two systems loiter until the crew arrives. The second launch delivers the crew in the CEV, which rendezvous with the EDS and LSAM. The EDS then performs the TLI burn. The LSAM performs both the LOI and descent burns, while the CEV remains in LLO unmanned. After the surface mission, the crew ascends to the CEV and discards the ascent module of the LSAM. The CEV service module then performs the TEI burn to return directly to Earth. This is the system architecture that was selected during ESAS and is used as the baseline throughout this analysis.

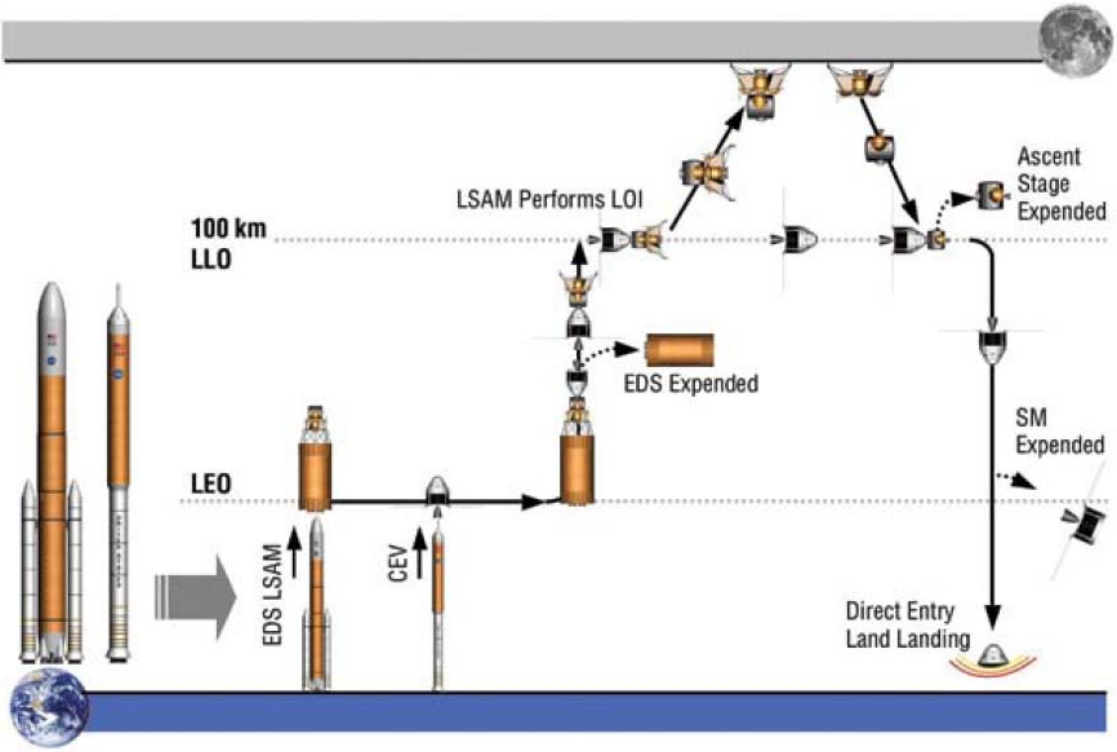

Figure 18: 1.5-Launch EOR-LOR System Architecture Option [8]

The third system architecture, presented in Figure 19, is an EOR-Direct system architecture that does not rendezvous in LLO at any time. The first two launches deliver two EDSs to LEO. The third launch delivers the crew in the CEV and a descent stage, which rendezvous with the two EDSs. In this architecture, the CEV will serve as the surface habitat and ascent stage. The EDSs then combine to perform the TLI and LOI burns. The descent stage performs the descent burn, and the crew lives in the CEV during the surface mission. After the surface mission, the crew ascends, using the CEV SM to perform both the ascent and TEI burns to return directly to Earth.

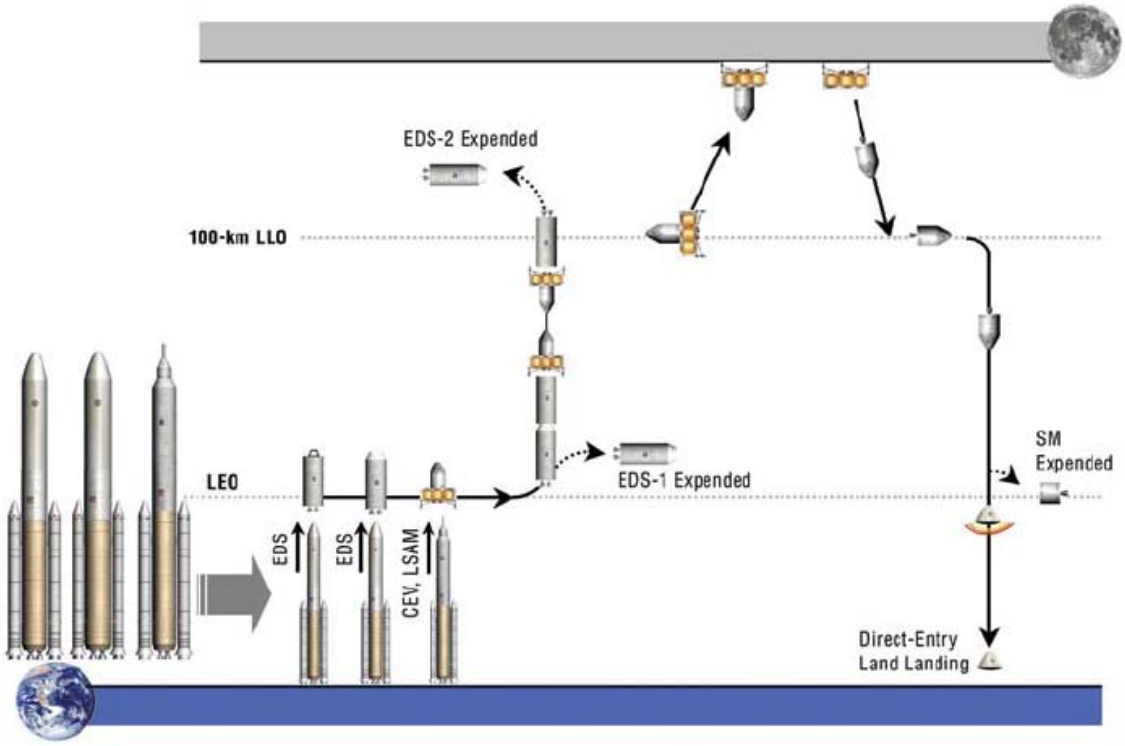

Figure 19: EOR-Direct System Architecture Option [8]

The fourth and final system architecture presented in ESAS, presented in Figure 20, is a modified EOR-Direct system architecture that leaves the CEV service module in LLO while crew still uses the capsule as the surface habitation. The first two launches deliver two EDSs to LEO. The third launch delivers the crew in the CEV, a descent stage, and an ascent stage, which rendezvous with the two EDSs in LEO. The EDSs again combine to perform the TLI and LOI burns. The descent stage performs the descent burn, and the crew lives in the CEV during the surface mission. In this system architecture, the CEV service module remains in LLO. After the surface mission, the crew ascends using the ascent stage, rendezvous with the CEV service module. The CEV service module then performs the TEI burn and the crew returns directly to Earth.

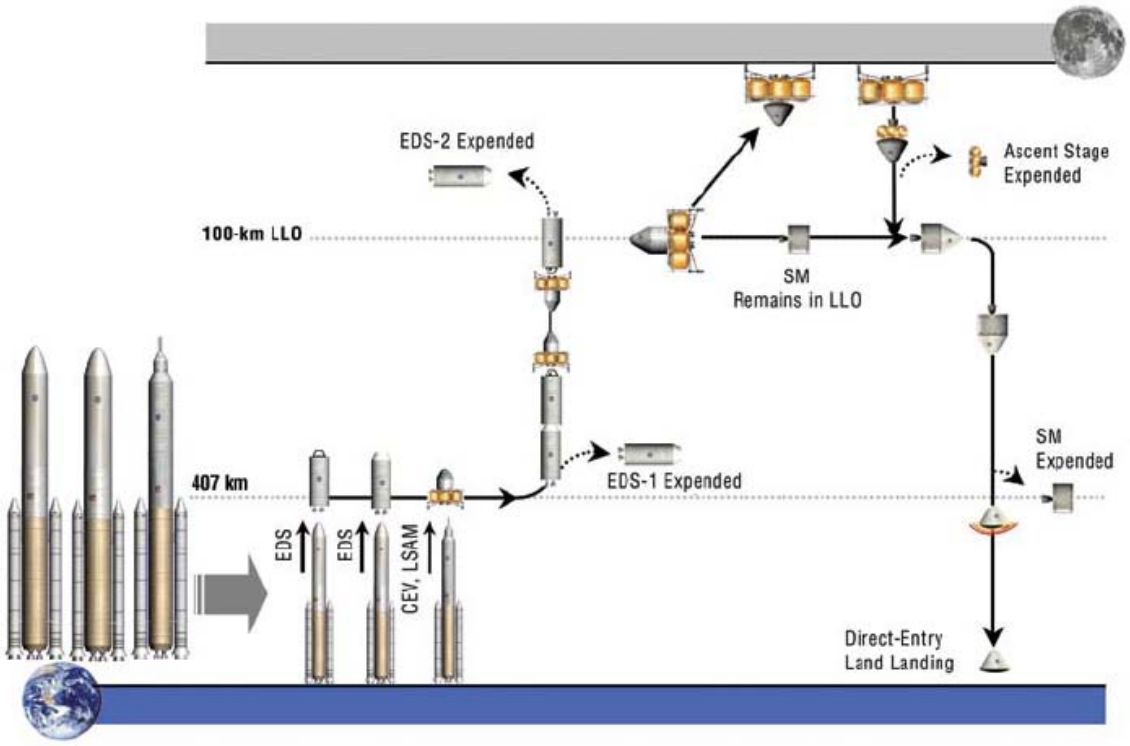

Figure 20: Modified EOR-Direct (SM Remains in LLO) System Architecture Option [8]

To supplement these system architectures and to test the flexibility of the modeling framework and system-level CERs, another system architecture type was added to the trade space. The system architecture, presented in Figure 21, is an EOR-LOR mission that utilizes commercial launch vehicles and on-orbit refueling [16]. This architecture type is significantly different than the architectures presented in ESAS which utilize HLLVs and do not include on-orbit refueling.

In this system architecture, a commercial launch vehicle (in this case, the Falcon Heavy under development by Space Exploration Technologies (SpaceX)) delivers a propellant depot to LEO. Then, propellant is transferred into the depot using subsequent commercial launches. Once the propellant depot is filled, an EDS is delivered to LEO, which receives all the propellant that was stored in the propellant depot. The next launch delivers the CEV and a two-stage LSAM to LEO. In this system architecture, the crew can be launched in the CEV or utilize a commercial crew launch capability and transfer into the CEV on orbit. From LEO, the EDS performs the TLI and LOI burns. The CEV remains in LLO while the crew performs the surface mission in the LSAM. After the surface mission, the crew ascends to the CEV and discards the ascent module of the LSAM. The CEV service module then performs the TEI burn to return directly to Earth.

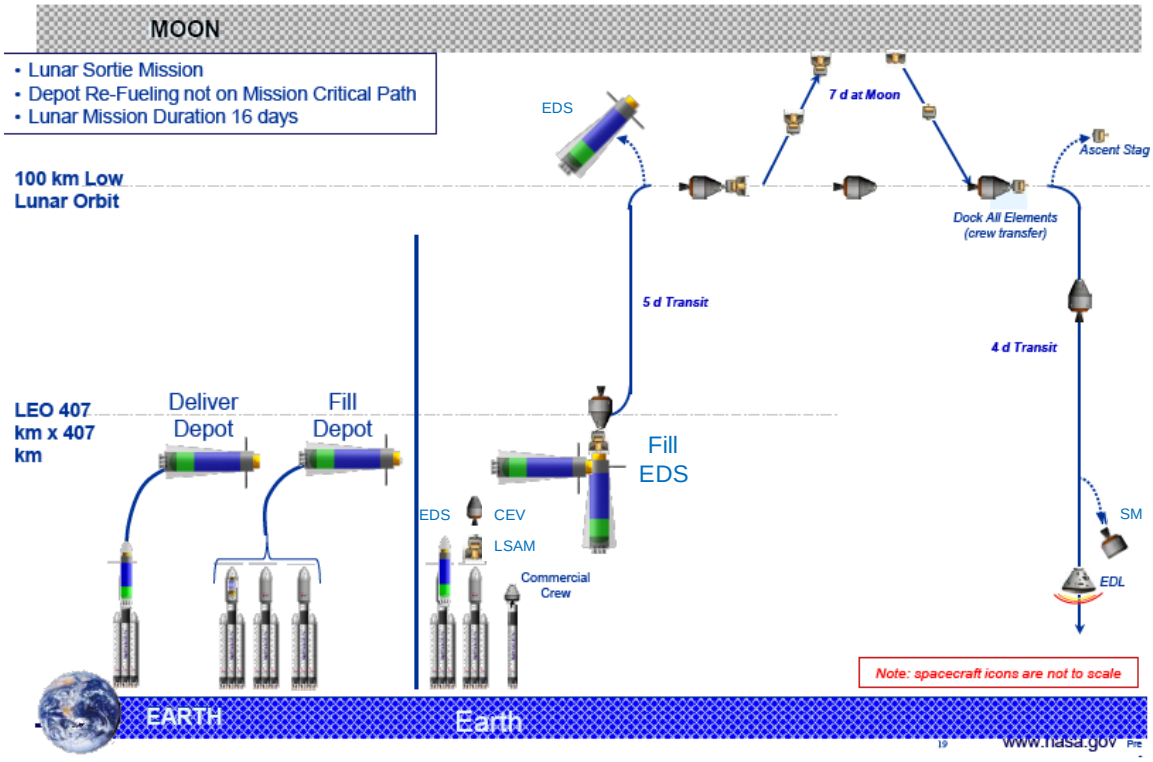

Figure 21: EOR-LOR System Architecture with On-Orbit Refueling and Commercial Launch Vehicles [16]

B. Analysis Results

The lunar system architectures above were analyzed using the modeling framework, providing estimates of mass, cost, and relative net present value (which incorporates discounting and inflation to account for the time value of money). Beyond the architecture options, propellant type was also varied. ESAS selected Liquid Oxygen (LOX)/Methane (CH4) propellant for the CEV and LSAM to promote commonality with Mars missions with in-situ resource utilization. The present framework also permits the exploration of multiple propellant types, such as Nitrogen Tetroxide (NTO)/Monomethylhydrazine (MMH). The complete design space is presented in Table 5. The results and a discussion on the validity of the analysis results are presented in the following section.

Table 5: Overview of Architecture Options (Bold Text Indicates Baseline)

No.	Mode	EDS Propellant	CEV SM Propellant	Ascent Stage Propellant
1	LOR-LOR	LOX/LH2	LOX/CH4	LOX/CH4
2	LOR-LOR	LOX/LH2	NTO/MMH	NTO/MMH
3	**1.5-Launch EOR-LOR**	**LOX/LH2**	**LOX/CH4**	**LOX/CH4**
4	1.5-Launch EOR-LOR	LOX/LH2	NTO/MMH	NTO/MMH
5	1.5-Launch EOR-LOR	LOX/CH4	LOX/CH4	LOX/CH4
6	EOR-Direct	LOX/LH2	LOX/CH4	LOX/CH4
7	EOR-Direct	LOX/LH2	NTO/MMH	NTO/MMH
8	EOR-Direct (SM in LLO)	LOX/LH2	LOX/CH4	LOX/CH4
9	EOR-Direct (SM in LLO)	LOX/LH2	NTO/MMH	NTO/MMH
10	Commercial with Depots	LOX/LH2	LOX/CH4	LOX/CH4
11	Commercial with Depots	LOX/LH2	NTO/MMH	NTO/MMH

While system architecture number 5 is functionally feasible as defined above, it is physically infeasible due to the relatively low specific impulse of LOX/CH4 stages when compared to LOX/Liquid Hydrogen (LH2). The larger propulsive stages resulting in the use of LOX/CH4 propellant do not fit into any launch vehicle option included in the graph. Note that the launch vehicles used in this analysis have a fixed LEO payload delivery capability, while the propulsive stages were sized to meet the functional requirements of the system architecture. Also, a single launch vehicle system can represent multiple launch vehicles if the payloads must be divided onto multiple flights.

The modeling framework does not include the DDT&E cost of a launch vehicle system if a similarly sized launch vehicle is already developed for a given system architecture. The two LOR-LOR architectures (numbers 1 and 2) only have two launches, but the launch vehicle is the 130 mt HLLV. The four EOR-Direct architectures (numbers 7, 8, 9, and 10) use three launches of the smaller 100 mt HLLV. The 1.5-launch architectures (numbers 3, 4, and 5) utilize the 150 mt HLLV, which stages at a suborbital point. The EDS must perform the rest of the ascent ΔV in addition to its in-space burns.

Figure 22 presents a comparison of the Initial Mass in Low Earth Orbit (IMLEO) and relative cost for each system architecture (as compared to the baseline system architecture, 3). The IMLEO is the total mass of the systems including the refueled propellant, but not including the launch vehicles and suborbital propellant. Note that there is no clear trend between IMLEO and cost. The refueling architectures that use commercial launch vehicles have the lowest cost, but also have the highest IMLEO. Alternatively, the LOR-LOR architectures have the lowest IMLEO, but have higher cost than many system architectures with higher IMLEO. Overall, this plot shows distinct levels of cost for each launch vehicle type—Falcon Heavy (10 and 11), 100 mt HLLV (6, 7, 8, and 9), 130 mt HLLV (1 and 2), and 150 mt HLLV with 29 mt crew launch vehicle (3 and 4). The larger HLLV DDT&E and flight unit costs increase the overall architecture cost while the commercial launch vehicles provide significant cost savings due to their low flight unit costs and no DDT&E cost. Alternatively, system architecture decisions such as propellant type have a relatively small impact on cost.

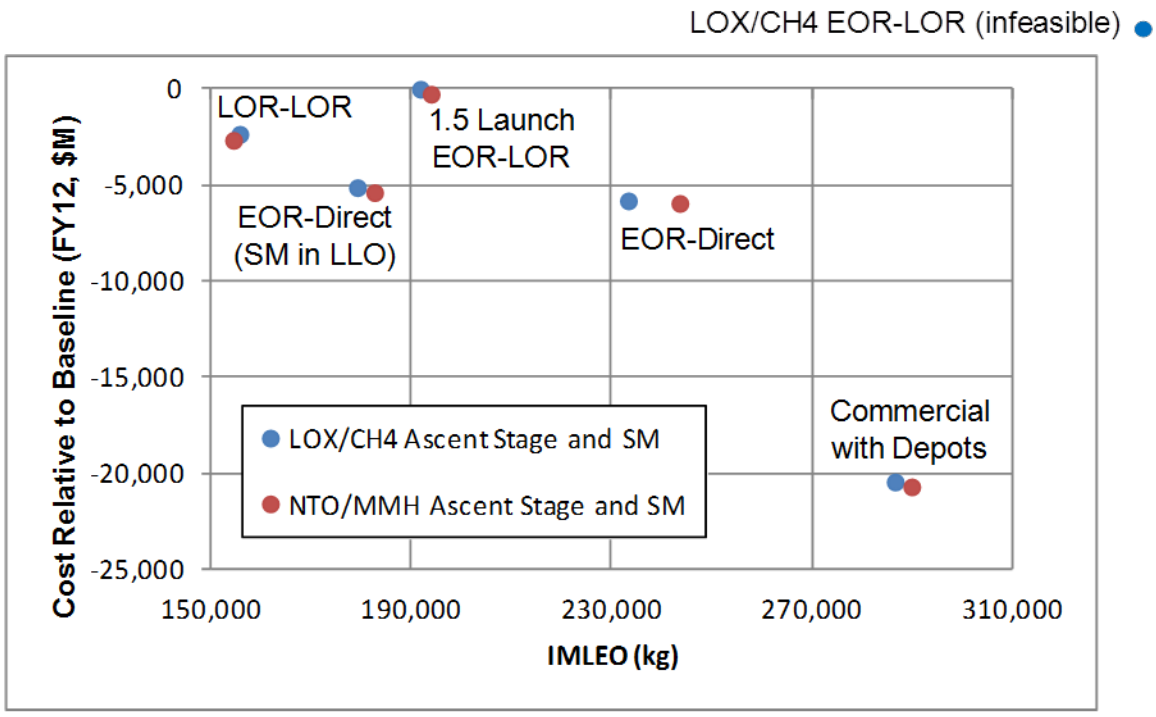

Figure 22: Mass and Cost Comparison for ESAS Mode Analysis

The difference between the IMLEO in system architectures 6 and 7 is larger because changes in the ascent/TEI combo stage has a very high impact on all of the systems lower in the system hierarchy compared to the architectures that use single-use systems (separate ascent and TEI stages). In stages that perform smaller ΔVs, the Inert Mass Fraction (IMF) is increasingly more impactful on gross mass. Therefore, switching propellants on the ascent stage and CEV service module propellants to NTO/MMH, which has lower *Isp* and higher IMF, increases the gross mass of the larger stage more. This increase in system mass also increases the payload mass for the stages

lower in the system hierarchy. The larger change in the ascent/TEI combo stage mass in architecture 7 over architecture 6 (EOR-Direct architectures), therefore, produces a larger increase in IMLEO as compared to the other system architecture pairs.

Figure 23 separates the overall cost into its components of DDT&E cost and flight unit cost. The pairs of points indicate the different architecture modes presented above, and the difference between the two points within a given pair represents the difference in cost for changing the ascent stage and CEV service module from LOX/CH4 to NTO/MMH. It is noteworthy that the data plotted does not include flight rate and learning effects on mission cost. These effects exist over multiple missions to a given destination and for missions that use multiples of a given system.

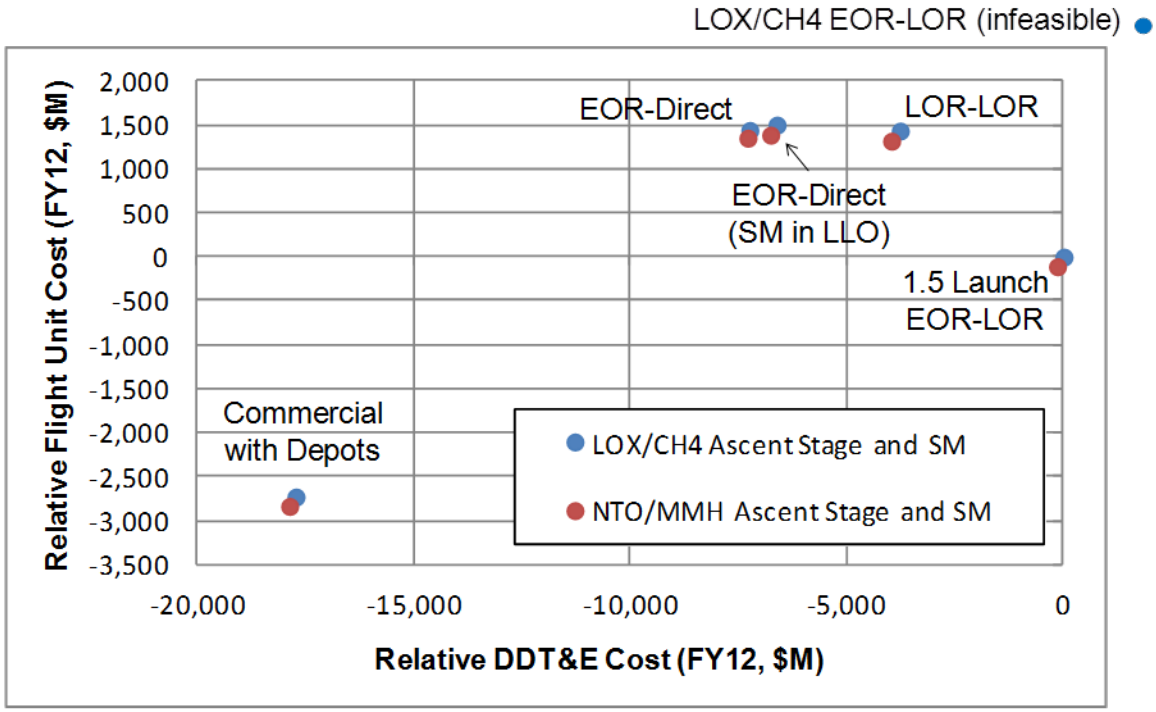

Figure 23: Relative DDT&E and Flight Unit Costs for ESAS Mode Analysis

In every case, NTO/MMH propellant provides a savings in cost, although this change is very small compared to the changes between the system architecture modes. The overall cost only considers DDT&E and flight unit costs; however, the toxicity of NTO/MMH would have a significant impact on the operations cost of an architecture. This impact would need to be quantified before this architecture decision was made. The baseline EOR-LOR system architectures (3 and 4) have the lowest flight unit cost of any of the ESAS architectures that utilize an HLLV. However, these architectures also have the highest DDT&E cost of any architecture. Using the smaller HLLV reduces the DDT&E cost, but the flight unit cost is very similar for the system architectures that use HLLVs. The baseline architectures use a combination of HLLV and a crew launch vehicle, which reduces the flight unit cost. Finally, the commercial launch architecture with propellant refueling provides significant savings in both DDT&E and flight unit costs.

The results in Figure 23 show that the LOR-LOR and both EOR-Direct architectures have higher flight unit cost and lower DDT&E cost than the baseline. The DDT&E cost for the LOR-LOR architectures is approximately $3-4B more than the EOR-Direct architectures because of the number of systems and the launch vehicle selection. The increased DDT&E cost of a surface habitat (approximately $2.0B) and TEI stage/CEV service module (approximately $1.2B), as well as an extra $2B in DDT&E cost for the 130 mt HLLV over a 100 mt HLLV, contribute to the total cost increase. These increases are offset by a smaller ascent stage, descent stage, and TLI/LOI stages for the LOR-LOR architectures. Finally, the EOR-Direct architectures that leave the CEV service module in LLO have a slightly higher DDT&E cost because of the additional system (ascent stage and TEI stage/CEV service module are separated). While the two systems are smaller, the development of two smaller systems is more expensive than one larger system.

All of the LOR-LOR and EOR-Direct architectures (1, 2, 6, 7, 8, and 9) have a similar flight unit cost. All are approximately $1.5B more than the baseline architecture in flight unit cost. Two launches of the 130 mt HLLV (LOR-LOR architectures) is approximately $5.6B, while three launches of the 100 mt HLLV (EOR-Direct architectures) is approximately $6.0B. The elimination of systems in the EOR-Direct architectures reduces the flight unit cost to equalize these two system architecture modes. Not coincidentally, the additional cost for the LOR-LOR and EOR-Direct architectures is primarily driven by the difference between the cost of the 29 mt crew launch vehicle and an HLLV. The launch cost for the EOR-LOR architectures is approximately $3.9B.

More significant than the savings from any of the HLLV-based architectures is the savings realized by using commercial launch vehicles (10 and 11). The elimination of approximately $15-21B of launch vehicle DDT&E cost by using commercial launch vehicles is clearly seen in Figure 23. Also, the flight unit cost for system architectures with commercial launch vehicles is reduced from $4-6B to hundreds of millions of dollars. It must also be acknowledged that the actual cost savings of the system architectures with commercial launch vehicles and refueling is not as large as the launch vehicle savings alone. This additional cost is due to the infrastructure that must be developed for on-orbit refueling (namely, a propellant depot).

Again, changes in the other system architecture decisions, such as rendezvous location and propellant type, have an order-of-magnitude smaller impact on the overall cost as compared to the launch vehicle selection. This is clearly shown in Figure 23 by comparing the magnitude of the cost difference between the propellant types for each system architecture pair. In every case, replacing LOX/CH4 on the CEV service module and ascent stage with NTO/MMH improves the cost. However, the difference is extremely small for a given system architecture, and the complications associated with the toxicity of that propellant must be considered before that decision is made. LOX/CH4 has a higher specific impulse than NTO/MMH, but a worse IMF (due to lower bulk density and cryogenic thermal control). For the smaller systems, these impacts offset, and the gross mass for the systems is similar. Therefore, the impact on the systems lower in the hierarchy is also minimal. The exception to this is when a propellant with a lower Isp is used for a large stage. This situation occurs in system architecture number 5, where LOX/LH2 is replaced by LOX/CH4, resulting in an infeasible solution. Also, as previously discussed, changing the ascent/TEI stage to NTO/MMH has a more significant impact than it does in other system architectures.

C. Validation

Based on the analysis performed using the modeling framework, the ESAS baseline system architecture does not have the best cost of the options analyzed in the ESAS trade space. The EOR-Direct architecture with the NTO/MMH ascent/TEI stage had the lowest cost of the options presented in ESAS. However, the Figures of Merit (FOMs) used to select the ESAS baseline architecture include factors beyond affordability. These were safety & mission success, effectiveness & performance, extensibility/flexibility, and programmatic risk [8].

As presented in the ESAS report and reproduced here in Figure 24, the selected EOR-LOR baseline system architecture has the lowest probability of Loss of Crew (LOC) of the analyzed options, making it the best option of the ESAS modes with respect to the safety & mission success FOM [8]. The graphical representation of the system architecture design space enforces that the same mission objectives (surface payload, crew size, surface duration, etc.) are accomplished by each architecture. Therefore, the effectiveness & performance FOM is not a discriminator between architectures.

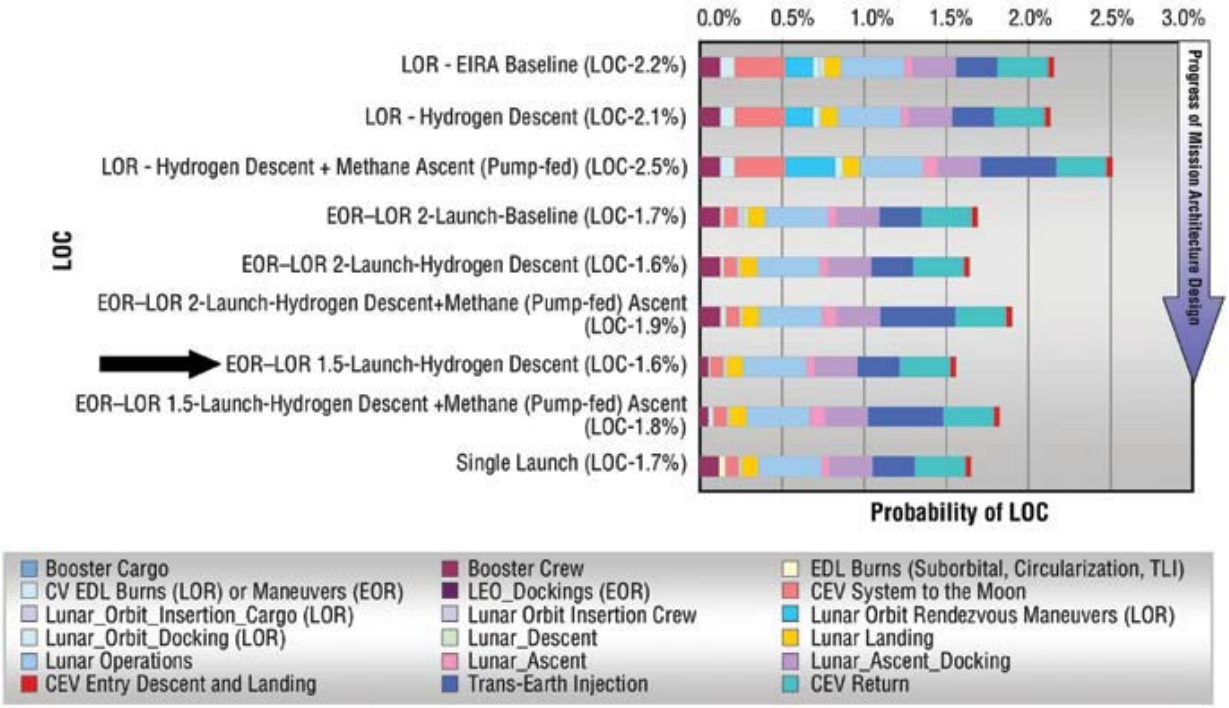

Figure 24: Loss of Crew (LOC) FOM Comparison from ESAS Mission Modes [8]

The selection of LOX/CH4 propellant usage in the ascent stage and the CEV SM relate directly to the extensibility/flexibility FOM. The use of In-Situ Resource Utilization (ISRU) at Mars commonly produces oxygen and methane for consumables and propellant. Also, developing a large launch vehicle would be useful to deliver the required payloads for a human Mars mission. The baseline architecture develops the largest of the launch vehicles.

Also, one of the requirements during ESAS was to deliver crew to the International Space Station (ISS) as quickly as possible to accommodate the retirement of the Space Shuttle. Therefore, the near-term development of a small crew launch vehicle (later renamed Ares I) met that requirement, and it improved the programmatic risk by using Shuttle-derived hardware to create an initial capability that was still useful for human exploration while the HLLV was under development [8].

Finally, the results of the analysis performed using the modeling framework estimates the baseline EOR-LOR as the highest cost. This is primarily driven by the DDT&E cost, which is the highest of any of the system architectures analyzed. Alternatively, the baseline architecture has the lowest flight unit cost of the ESAS architecture options, which is beneficial for a continued campaign of lunar missions. The analysis presented in ESAS concludes that the estimated cost of all of the architectures is of a similar order of magnitude. The analysis performed with the modeling framework is consistent with this conclusion, for the system architecture that utilizes commercial launch vehicles has an order of magnitude lower cost than all of the system architectures that utilize HLLVs.

V. Conclusion

This paper presented a set of system-level cost estimating relationships for use in space system architecture design space exploration. These CERs were included in a architecture modeling framework that utilizes graph theory to model the locations, steady states, and functional options for a given mission. This framework was used to analyze the ESAS mission modes comparison along with another system architecture that is significantly different. The use of the system-level CERs enables rapid estimation of DDT&E and flight unit costs for each system within the architecture, which, had this capability been available at the time, could have been used to qualitatively compare the different architecture options.

During the space system architecture design space exploration phase, incorporating cost into the decision-making is a valuable addition to the amount of knowledge that typically relies on qualitative information and basic quantitative information. By creating the system-level CERs presented in this paper, approximate cost data can be created for systems that have very little fidelity, enabling relative cost comparisons between system architecture options. Often, system architectures within a given design space are vastly different (such as the ESAS architectures

and the commercial architecture with refueling), but a consistent means with which to create estimates for development and flight unit costs enable credible relative comparisons.

Acknowledgments

The authors would like to acknowledge the encouragement and support by the Space Mission Analysis Branch at NASA Langley Research Center. Their interest in developing the capability to explore the space system architecture design space has prompted the authors to continue advancing this field into the future.

References

1. 2008 NASA Cost Estimating Handbook. NASA Headquarters Cost Analysis Division, 2008.
2. Krevor, Zachary C. *A Case Study of the STS Indirect and Support Costs: Lessons to be Learned for the Next Generation Launch System.* AE 8900 Project, Georgia Institute of Technology. April 2004.
3. Young, David A. *An Innovated Method for Allocating Reliability and Cost in a Lunar Exploration Architecture*. Ph.D. Dissertation, Georgia Institute of Technology. May 2007.
4. McAfee, Julie, Culver, George, and Naderi, Mahmoud. *NASA/Air Force Cost Model (NAFCOM): Capabilities and Results*. 2011 JANNAF MSS/LPS/SPS Meeting, Huntsville, AL. December 2011.
5. Koelle, Dietrich E. *Handbook of Cost Engineering for Space Transportation Systems (Revision 2) with Transcost 7.1 Statistical-Analytical Model for Cost Estimation and Economical Optimization of Launch* Vehicles. TCS-TransCostSystems. Ottobrunn, Liebigweg, Germany. February 2006.
6. Shishko, Robert. *NASA Systems Engineering Handbook*. NASA SP-610S, June 1995.
7. Arney, Dale C. *Rule-Based Graph Theory to Enable Exploration of the Space System Architecture Design Space*. Ph.D. Dissertation, Georgia Institute of Technology. August 2012.
8. *NASA's Exploration Systems Architecture Study Final Report*. NASA TM-2005-214062. November 2005.
9. Heineman, Jr., Willie. *Design Mass Properties II: Mass Estimating and Forecasting for Aerospace Vehicles Based on Historical Data*. JSC-26098. November 1994.
10. Isakowitz, S., Hopkins, J., and Hopkins, Jr., J. *International Reference Guide to Space Launch Systems, 4th Ed*. AIAA, 2004.
11. Human Architecture Team Steering Council. *HEFT Phase I Closeout*. NASA Internal Study, September 2010.
12. Young, James J. *A Value Proposition for Lunar Architectures Utilizing On-Orbit Propellant Refueling*. Ph.D. Dissertation, Georgia Institute of Technology. May 2009.
13. Falcon Heavy Website, Space Exploration Technologies Website, URL: <http://www.spacex.com/falcon_heavy.php>. Accessed May 27, 2012.
14. West, Douglas B. *Introduction to Graph Theory*. Prentice Hall: Upper Saddle River, NJ. 1996.
15. Arney, Dale and Wilhite, Alan. "A Flexible Modeling Environment for Evaluating Space System Architectures." AIAA Paper No. 2010-8107, August 2010.
16. Wilhite, Alan, Stanley, Douglas, Arney, Dale, and Jones, Chris. "Near Term Space Exploration with Commercial Launch Vehicles plus Propellant Depot." March 2011. URL: <http://nasawatch.com/archives/2011/03/using-commercia.html>. Accessed May 27, 2012.